# Analytical description of the flux-flow mode in a long Josephson junction

Marek Jaworski
*Institute of Physics and College of Science, Polish Academy of Sciences, Al. Lotników 32/46, 02-668 Warszawa, Poland*
(Received 5 February 1999)

The flux-flow mode in a long one-dimensional Josephson junction is studied analytically. An approximate steady-state solution of the perturbed sine-Gordon equation is derived in the form of a dense fluxon chain accompanied by small-amplitude plasma waves. Next, some time-averaged quantities are calculated, making it possible to evaluate the constant bias current and the constant voltage between the junction electrodes. The analytical results are compared with numerical simulations both for the field distribution within the junction and for the *I-V* characteristics. [S0163-1829(99)12533-5]

## I. INTRODUCTION

The flux-flow (FF) mode was suggested more than a decade ago[1] as a simple mechanism of multifluxon propagation in a long one-dimensional Josephson junction. The FF mode appears for a sufficiently large external magnetic field applied in the junction plane, and can be described briefly as a unidirectional viscous flow of fluxons, created at one end of the junction and annihilated at the other.

Since the first publications on the FF phenomena, the Josephson junction operated in the FF mode has attracted considerable attention in view of possible applications, e.g., as a local oscillator for integrated submillimeter-wave receivers.[2,3] On the other hand, the FF mode is also of theoretical interest, since multiperiodic solutions of the underlying sine-Gordon equation have not been thoroughly studied so far.

Contrary to many experimental papers on FF phenomena, the theoretical results are scarce and confined mainly to direct numerical simulations[1,4] or infinite expansions with respect to linear cavity modes.[5] On the other hand, a purely analytical approach is based on the traveling-wave approximation, thus ignoring the boundary effects.[6,7] In this connection, when many results (mainly experimental and numerical) have already been published, there is a need for an adequate analytical model, making it possible to describe the mechanism of the FF propagation in a long junction of finite length.

In the present paper we discuss such a simple model, making use of exact multiperiodic solutions of the sine-Gordon equation, reported recently.[8] The boundary conditions are satisfied by the FF mode interacting with small-amplitude plasma waves. The steady-state solution taking into account bias and losses is obtained by a simple perturbation scheme, based on the energy balance.[9,10]

The paper is organized in the following way: Approximate analytical solutions of the perturbed sine-Gordon equations are discussed in Sec. II. This section contains the main result of the paper, i.e., the approximate steady-state solution satisfying appropriate boundary conditions at the junction edges. The approximate solution is then used in Sec. III to evaluate some time-averaged quantities, like the constant current and the constant voltage measured across the junction. In Sec. IV analytical results are compared with numerical data, both for the field patterns within the junction and for the *I-V* characteristics. Section V contains summary of the results; we discuss also some open problems and possible generalizations of the method.

## II. FORMULATION OF THE PROBLEM AND APPROXIMATE ANALYTICAL SOLUTIONS

Fluxon dynamics in a long one-dimensional Josephson junction is described by the perturbed sine-Gordon equation[9–11]

$$\phi_{xx}-\phi_{tt}=\sin\phi+\alpha\phi_t-\gamma, \tag{1}$$

where $\phi$ denotes the quantum phase difference between the junction electrodes, $\alpha$ is the dissipation coefficient, and $\gamma$ is the normalized bias current density. The above equation is written in the dimensionless form such that the spatial coordinate $x$ is normalized to the Josephson penetration depth $\lambda_J$ and time $t$ to the inverse plasma frequency $\omega_0^{-1}$. We consider a long junction, i.e., satisfying the relation $L\gg 1$, where $L$ is the normalized junction length.

The boundary conditions depend on the electrode geometry, and for the overlap structure can be written as[11]

$$\phi_x(-L/2)=h, \tag{2a}$$

$$\phi_x(L/2)=h, \tag{2b}$$

where $h$ denotes the normalized external magnetic field. In the overlap geometry we neglect the self-field effects, and the bias current density $\gamma$ follows from the aproximation of the transversal field distribution in a real (two-dimensional) junction.[11]

Let us consider first the lossless case ($\alpha=0,\gamma=0$), for which the exact analytical solutions of Eq. (1) are known.[12] It can be shown[8] that the unidirectional flow of solitons (fluxons) in the limit of a ''dense soliton train'' is described approximately as

$$\phi=Q(kx+\omega t)-4q\sin[Q(kx+\omega t)]+\mathcal{O}(q^2), \tag{3}$$

where $Q\gg 1$, $q=\exp(-Q\pi/2)\ll 1$, and the dispersion relation is

$$4qQ^2(k^2-\omega^2)=1. \tag{4}$$

 

The normalized magnetic field within the junction is given by $\phi_x$:

$$\phi_x = Qk - 4qQk\cos[Q(kx+\omega t)] + \mathcal{O}(q^2). \tag{5}$$

Using the dispersion relation (4) and denoting the external magnetic field as $h = Qk$ we obtain

$$\phi_x = h - \frac{1}{h(1-v^2)}\cos[h(x+vt)] + \mathcal{O}(q^2), \tag{6}$$

where $v = \omega/k$ and $1-v^2$ is the usual Lorentz factor.

One can see that the above simple expression reproduces well all the characteristic features of the FF mode discussed in the literature.[4] In particular, we obtain a dense train of overlapping fluxons separated by $2\pi/h$. As the external magnetic field $h$ increases, the fluxon train becomes more dense and its amplitude decreases.

It is clear, however, that the boundary conditions (2) cannot be satisfied by the solution (6), since apart from the constant term $h$ it contains also the oscillatory term. Therefore we have to consider a more complicated solution of Eq. (1), which in the lossless case describes the interaction of the fluxon train with quasilinear plasma waves. In the limit of small amplitudes both interacting excitations (i.e., fluxon train and plasma wave) enter the formalism additively and we have[8]

$$\phi = Q(kx+\omega t) - 4q\sin[Q(kx+\omega t)] + p\sin(\kappa x+\Omega t+\Theta) + \mathcal{O}(q^2,p^2), \tag{7}$$

where $k$ and $\omega$ are related by the dispersion Eq. (4), as before, $p$, $\Theta$ denote the amplitude and phase of the plasma wave, respectively, while the dispersion parameters $\kappa$ and $\Omega$ satisfy the relation $\kappa = \pm\Omega$.

In other words, the unidirectional fluxon train is accompanied by plasma waves of arbitrary frequency, propagating in both directions with a critical velocity (corresponding to the normalized Swihart velocity) $\Omega/\kappa = \pm 1$. It will be shown later that the proper choice of the amplitudes and phases of two plasma waves propagating in opposite directions makes it possible to satisfy exactly the boundary conditions (2).

Let us consider now the case with bias and damping, i.e., the full perturbed Eq. (1). We assume the solution to be (multi)periodic, but allow both amplitudes and phases to depend slowly on $x$. Replacing $Qkx$ by $\vartheta(x)$ and $\kappa x$ by $\mu(x)$ we can write the most general ansatz in the form

$$\phi = \vartheta(x) + Q\omega t - 4q(x)\sin[\vartheta(x)+Q\omega t] + p(x)\sin[\mu(x)+\Omega t+\Theta] + \mathcal{O}(q^2,p^2). \tag{8}$$

Substituting Eq. (8) into Eq. (1) and comparing two most dominant terms for $q$ and $p$ we find

$$\vartheta_{xx} - \alpha Q\omega = -\gamma, \tag{9a}$$

$$4q[(\vartheta_x)^2 - (Q\omega)^2] - 4q_{xx} = 1, \tag{9b}$$

$$p_{xx} - p(\mu_x)^2 + p\Omega^2 = 0, \tag{9c}$$

$$2p_x\mu_x + p\mu_{xx} - p\alpha\Omega = 0. \tag{9d}$$

The simplest solution of the above system of equations yields

$$q(x) = \text{const}, \tag{10a}$$

$$\vartheta(x) = Qkx, \tag{10b}$$

$$p(x) = pe^{\delta x}, \tag{10c}$$

$$\mu(x) = \kappa x, \tag{10d}$$

and substituting the solution (10) into Eqs. (9) we obtain

$$\alpha Q\omega = \gamma, \tag{11a}$$

$$4qQ^2(k^2-\omega^2) = 1, \tag{11b}$$

$$\delta^2 - \kappa^2 + \Omega^2 = 0, \tag{11c}$$

$$2\delta\kappa = \alpha\Omega. \tag{11d}$$

The above equations describe the Ohmic current density, dispersion relation for the FF mode, dispersion relation for the damped plasma wave, and the relation between the damping factor $\delta$ and the loss factor $\alpha$, respectively.

Substituting Eqs. (10) back into the ansatz (8) we obtain finally the approximate solution of the perturbed sine-Gordon Eq. (1):

$$\phi = Q(kx+\omega t) - 4q\sin[Q(kx+\omega t)] + pe^{\delta x}\sin(\kappa x+\Omega t+\Theta) + \mathcal{O}(q^2,p^2). \tag{12}$$

Thus, in the first-order approximation, the term describing the FF mode remains unchanged as compared to the lossless case, while the only infuence of losses on the plasma wave is an exponential dependence of its amplitude.

Let us consider now the flux-flow mode accompanied by two plasma waves propagating in opposite directions. Since we are interested in a steady-state and strictly time-periodic solution, we assume additionally $\Omega = Q\omega$, i.e., we make the plasma-wave frequency equal to that of the FF mode. Denoting, as before, $Qk = h$ and neglecting the higher-order terms, we find

$$\phi \simeq hx + \Omega t - 4q\sin(hx+\Omega t) + p_1e^{\delta x}\sin(\kappa x+\Omega t+\Theta_1) + p_2e^{-\delta x}\sin(\kappa x-\Omega t+\Theta_2), \tag{13}$$

thus the space derivative $\phi_x$ is given by

$$\phi_x \simeq h - 4qh\cos(hx+\Omega t) + p_1\sqrt{\kappa^2+\delta^2}e^{\delta x}\cos(\kappa x+\Omega t+\Theta_1-\xi) + p_2\sqrt{\kappa^2+\delta^2}e^{-\delta x}\cos(\kappa x-\Omega t+\Theta_2+\xi), \tag{14}$$

where $\xi = \arctan(\delta/\kappa)$.

For given parameters $h$ and $\Omega$, $q$ follows directly from the dispersion relation (4), thus Eq. (14) has four degrees of freedom: $p_1, p_2, \Theta_1, \Theta_2$. It can be easily shown that a proper choice of these parameters enables the boundary conditions (2) to be satisfied for arbitrary $t$.

Lengthy and tedious calculations will not be quoted here, we present only the final results:

$$p_2^1 = 4qh\frac{r}{(\kappa^2+\delta^2)^{1/2}}\left\{\frac{1-2r^2\cos[(h\pm\kappa)L]+r^4}{1-2r^4\cos 2\kappa L+r^8}\right\}^{1/2}, \tag{15a}$$

$$\Theta_2^1 = \arctan\frac{(1-r^6)\sin[(h\mp\kappa)L/2]+r^2(1-r^2)\sin[(h\pm 3\kappa)L/2]}{(1+r^6)\cos[(h\mp\kappa)L/2]-r^2(1+r^2)\cos[(h\pm 3\kappa)L/2]}\pm\xi, \tag{15b}$$

where $r=\exp(-\delta L/2)$, and the upper (lower) sign corresponds to the index 1 (2), respectively.

### III. CURRENT-VOLTAGE CHARACTERISTICS

Having derived the approximate solution (13) satisfying appropriate boundary conditions (2) we are in a position to discuss some time-averaged, directly measurable quantities, like the total current flowing through the junction and the constant voltage between the electrodes. To calculate the current-voltage ($I$-$V$) characteristics we use a simple perturbation method based on the energy balance.[9,10]

Let us consider the Hamiltonian

$$\mathcal{H}=\int_{-L/2}^{L/2}\left[\frac{1}{2}\phi_x^2+\frac{1}{2}\phi_t^2+(1-\cos\phi)\right]dx. \tag{16}$$

Differentiating with respect to time and using Eq. (1) we find

$$\frac{d\mathcal{H}}{dt}=\int_{-L/2}^{L/2}(\gamma\phi_t-\alpha\phi_t^2)dx+\phi_x\phi_t|_{-L/2}^{L/2}. \tag{17}$$

According to earlier assumptions, we consider a steady-state and strictly periodic solution, hence the time-averaged change of energy must be zero:

$$\int_{-L/2}^{L/2}(\gamma\langle\phi_t\rangle-\alpha\langle\phi_t^2\rangle)dx+\langle\phi_x\phi_t\rangle|_{-L/2}^{L/2}=0, \tag{18}$$

where $\langle f(t)\rangle\equiv(1/T)\int_0^T f(t)dt$.

The time derivative of Eq. (13) is given by

$$\begin{aligned}\phi_t &\simeq \Omega[1-4q\cos(hx+\Omega t)+p_1e^{\delta x}\cos(\kappa x+\Omega t+\Theta_1)\\ &\quad -p_2e^{-\delta x}\cos(\kappa x-\Omega t+\Theta_2)]\\ &= \Omega[1+F(x)\cos\Omega t+G(x)\sin\Omega t]\end{aligned} \tag{19}$$

where

$$\begin{aligned}F(x) &= -4q\cos hx+p_1e^{\delta x}\cos(\kappa x+\Theta_1)\\ &\quad -p_2e^{-\delta x}\cos(\kappa x+\Theta_2),\\ G(x) &= 4q\sin hx-p_1e^{\delta x}\sin(\kappa x+\Theta_1)\\ &\quad -p_2e^{-\delta x}\sin(\kappa x+\Theta_2).\end{aligned}$$

It is clear that the average value of $\phi_t$, corresponding to the constant voltage, is $\langle\phi_t\rangle=\Omega$ for arbitrary $x$. On the other hand, the boundary conditions imply $\phi_x(-L/2)=\phi_x(L/2)=h$. Thus $\langle\phi_x\phi_t\rangle|_{-L/2}^{L/2}=0$ in Eq. (18), and the energy balance can be written as

$$\gamma\Omega L=\alpha\int_{-L/2}^{L/2}\langle\phi_t^2\rangle dx. \tag{20}$$

Calculating the average of $\phi_t^2$ we find

$$\langle\phi_t^2\rangle=\Omega^2\left[1+\frac{1}{2}F^2(x)+\frac{1}{2}G^2(x)\right]. \tag{21}$$

Thus substituting Eq. (21) into Eq. (20) and identifying the frequency $\Omega$ with the constant voltage $V$ we obtain finally

$$\gamma=\alpha V\left\{1+\frac{1}{2L}\int_{-L/2}^{L/2}[F^2(x)+G^2(x)]dx\right\}. \tag{22}$$

One can see that the total current density $\gamma$ consists of an Ohmic term and a small contribution following from a nonzero Josephson term. In the nonrelativistic region, when $v=\Omega/h\ll 1$, the quantities $F$ and $G$ are negligibly small and the total current is equal practically to the Ohmic term. However, in the relativistic limit ($v\to 1$), the coefficients $q,p_1,p_2$, and consequently $F$ and $G$, become larger. As a result, the integral contribution in Eq. (22) cannot be neglected, giving rise to the so-called FF step.

### IV. RESULTS AND DISCUSSION

In this section we compare analytical expressions derived above with numerical results, obtained by the finite-difference implicit scheme.[13] Examples of the magnetic field distribution within the long junction ($L=10$) are shown in Fig. 1 for different frequencies $\Omega$, corresponding to different velocities of the fluxon train (and consequently, different voltages on the $I$-$V$ characteristics). For the remaining parameters we take realistic values $h=6$, $\alpha=0.1$, typical for the FF mode. The solid line shows the analytical approximation [Eq. (14)], while the open circles — results of numerical simulations — are shown graphically in a discrete set of $x$ values.

Figure 1(a) shows a fluxon train for moderate velocity $v=0.665$, i.e., far below the relativistic limit. It is clear that the fluxon train is indeed dense, the average distance betwen adjacent maxima being 1.048, in good agreement with the theoretical prediction $2\pi/h=1.047$.[4] However, we can observe also a weak dependence of the amplitude on the $x$ coordinate, following from the interference of fluxons with plasma waves. The agreement between analytical and numerical results is excellent, we can see the analytical solution reproducing perfectly all the details of the numerical data.

Similar results are shown in Figs. 1(b) and (c) for higher velocities ($v=0.930$ and $v=0.977$), closer to the relativistic limit. One can see the effect of interference between fluxons and plasma waves to be much stronger than for Fig. 1(a).

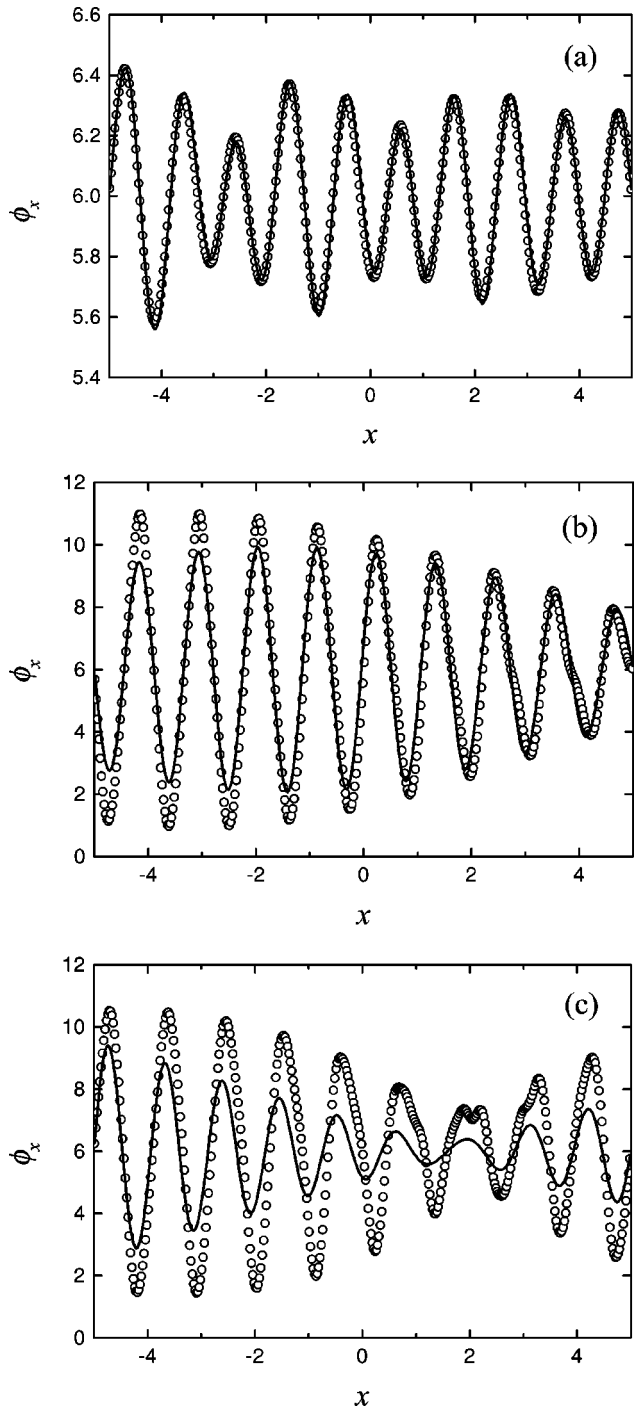


FIG. 1. Comparison of the analytical approximation (solid line) and the numerical results (open circles) for the magnetic-field distribution corresponding to different velocities of the fluxon train: (a) $v=0.665$, (b) $v=0.930$, (c) $v=0.977$. The remaining parameters are: $L=10$, $h=6$, $\alpha=0.1$.

Since in the relativistic limit ($v\to 1$) the propagation constant of the plasma wave $\kappa$ tends to that of the fluxon train (equal to $h$), a typical envelope pattern appears, similar to the interference of two waves of nearly equal frequencies. We can observe the agreement between theory and numerical results to be worse than in Fig. 1(a), nevertheless, the discrepancy is mainly confined to the amplitude, and all the qualitative features of the solution are reproduced correctly. [Note that the amplitudes are generally much larger than in Fig. 1(a).] A worse agreement of the results follows from the fact that in the relativistic limit the amplitudes $q,p_1,p_2$ become too large, and the approximate solution, being in fact an expansion with respect to small parameters, becomes less accurate. It should be noted here that without plasma waves taken into account we would have simply a traveling-wave approximation [Eq. (6)], i.e., an oscillatory solution of constant amplitude in the form of a cosine wave on the background of external magnetic field $h$. It is clear that such a solution does not satisfy the boundary conditions (2) and is not able to reproduce correctly the interference patterns shown in Figs. 1(a)–(c).

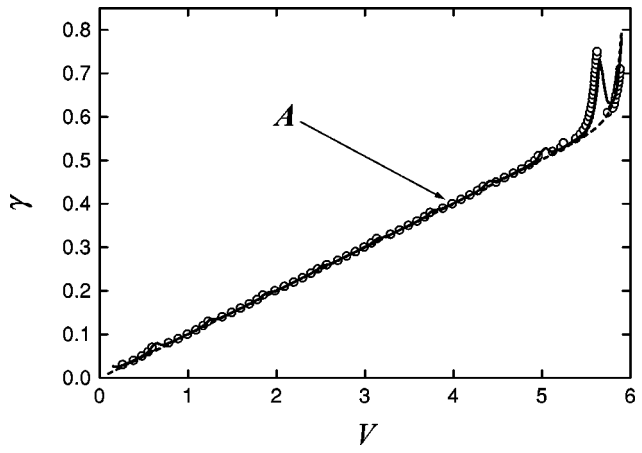


FIG. 2. $I$-$V$ characteristics calculated analytically (solid line) and numerically (open circles). The dashed line shows the traveling-wave approximation, i.e., the $I$-$V$ characteristic calculated without taking into account quasilinear plasma waves. The point $A$ corresponds to the field pattern shown in Fig. 1(a).

In Fig. 2 an analytically derived $I$-$V$ characteristic is compared with the results of direct numerical simulation. An analytical approximation (solid line) has been obtained by evaluating the current density $\gamma$ as a function of voltage $V$ according to Eq. (22). Numerical simulation (open circles) has been performed by solving Eq. (1) for given $\gamma$ and evaluating the average value of $\phi_t$ as $\langle\phi_t\rangle=[\phi(t+T)-\phi(t)]/T$ after a sufficiently long evolution when the time-dependent solution can be regarded as a steady state. For comparison, we show also the $I$-$V$ characteristic calculated within the traveling-wave approximation (dashed line) using Eq. (22) with $p_1=p_2=0$, thus ignoring the contribution from plasma waves. Figure 3 shows details of the $I$-$V$ characteristics and the hysteresis region in the vicinity of the FF step. The points $A$, $B$, and $C$ correspond to the magnetic-field distributions, shown in Figs. 1(a)–(c), respectively.

As before, in the nonrelativistic region (point $A$) the analytical approximation reproduces perfectly the numerically obtained $I$-$V$ characteristic, together with small but clearly visible maxima following from the interference of plasma waves. The accuracy becomes worse when we approach the relativistic limit (points $B$ and $C$), nevertheless we obtain at least qualitatively correct results for the hysteresis region. In particular, we can observe the main FF step at $V=h$ accompanied by a Fiske resonance at $V\simeq h-\pi/L$ with a segment of negative differential conductivity. This part of the characteristics is visible only in the analytical approximation, since for a sufficiently small loss factor $\alpha$ any solution within the

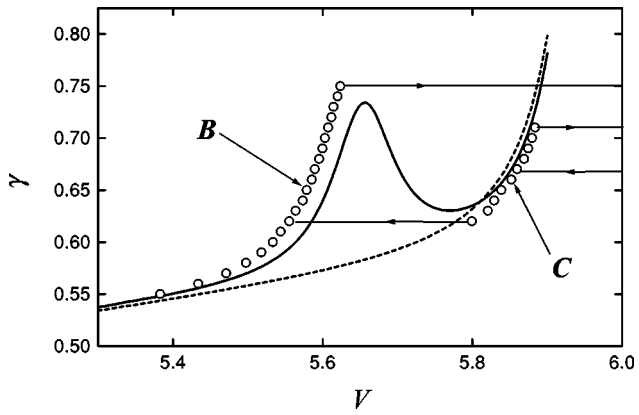


FIG. 3. Details of the *I*-*V* characteristics in the hysteresis region. The points *B* and *C* correspond to the field patterns shown in Figs. 1(b) and (c), respectively.

negative conductivity segment is unstable and cannot be obtained numerically. Similarly as in the case of magnetic field distributions (Fig. 1), a worse agreement of the results in the relativistic limit follows first of all from the fact that the amplitudes $q, p_1, p_2$ grow as we approach the FF step region, and the series expansions with respect to small parameters become slowly convergent.

We note also that neglecting the plasma waves results in a smooth and monotonic *I*-*V* dependence without a fine structure related to Fiske resonances. In other words, the traveling-wave approximation is not sufficient to describe correctly the *I*-*V* characteristic in the hysteresis region.

## V. SUMMARY AND CONCLUSIONS

In the present paper a simple analytical model has been proposed, making it possible to describe the FF mode propagating in a long one-dimensional Josephson junction. The model takes into account both bias and damping terms, present in the perturbed sine-Gordon Eq. (1). The boundary conditions are satisfied by an approximate solution in which the unidirectional fluxon train is accompanied by two plasma waves propagating in opposite directions with a velocity $\Omega/\kappa \simeq 1$. Analytical approximation, in turn, allows some experimental quantities like current and voltage to be evaluated and compared with the results of direct numerical simulations.

The comparison shows an excellent agreement in the nonrelativistic region, both in the case of field patterns within the junction [Fig. 1(a)] and in the current-voltage characteristics. In the relativistic limit we observe some discrepancy between analytical and numerical results. Nevertheless, owing to the analytical approximation it is possible not only to reproduce (at least qualitatively) the hysteresis region, but also to determine a segment of negative conductivity in the *I*-*V* characteristic. It seems that such a segment can be directly responsible for various important parameters of the FF oscillator such as the linewidth, stability, etc. Thus a more detailed analysis of the *I*-*V* characteristic in the vicinity of the FF step is needed, in view of possible applications in superconducting electronics.

It should be stressed, however, that the consistency and agreement between analytical and numerical results does not mean that the one-dimensional model is adequate for the description of a real three-dimensional structure. As shown in Ref. 11, the overlap structure can be effectively reduced to the one-dimensional model, provided the bias current density $\gamma$ is small and evenly distributed along the junction. Unfortunately, in the vicinity of the FF step the current grows rapidly and the ''smallness'' condition may be violated. On the other hand, as shown in several papers dealing with static phenomena,[14,15] the current density distribution is not uniform but exhibits sharp maxima at the junction edges. One could expect the constant current density in the dynamical (time-dependent) state to be also nonuniform, thus it seems that the problem of current distribution, (and more generally, the problem of reducing a real junction to a one-dimensional model) requires further investigation.

Finally, it is worthwhile to note that the formalism developed in the present paper is not restricted to a single overlap junction. Preliminary results for the ''in-line'' geometry (with the self-field taken into account) show again an excellent agreement between analytical approximation and numerical data. On the other hand, the approximate solution derived here can be considered as a starting point in the analysis of more advanced structures, such as, e.g., stacked junctions investigated extensively over the last years.

## ACKNOWLEDGMENTS

The author wishes to thank Professor J. Zagrodziński for fruitful and stimulating discussions. This work was supported by the KBN Grant Nos. 2P03B 114-11 and 2P03B 148-14.

[1] T. Nagatsuma, K. Enpuku, F. Irie, and K. Yoshida, J. Appl. Phys. **54**, 3302 (1983); see also **56**, 3284 (1984); **58**, 441 (1985); **63**, 1130 (1988).
[2] V.P. Koshelets, A.V. Shchukin, S.V. Shitov, and L.V. Filippenko, IEEE Trans. Appl. Supercond. **3**, 2524 (1993).
[3] J. Mygind, V.P. Koshelets, A.V. Shchukin, S.V. Shitov, and I.L. Lapytskaya, IEEE Trans. Appl. Supercond. **5**, 2951 (1995).
[4] O.H. Olsen, A.V. Ustinov, and N.F. Pedersen, Phys. Rev. B **48**, 13 133 (1993).
[5] M. Cirillo, N. Grønbech-Jensen, M.R. Samuelsen, M. Salerno, and G. Verona Rinati, Phys. Rev. B **58**, 12 377 (1998).
[6] P.M. Marcus and Y. Imry, Solid State Commun. **33**, 345 (1980).
[7] R.D. Parmentier, P. Barbara, G. Costabile, A. D'Anna, B.A. Malomed, and C. Soriano, Phys. Rev. B **55**, 15 165 (1997).
[8] M. Jaworski, Phys. Lett. A **244**, 97 (1998).
[9] D.W. McLaughlin and A.C. Scott, Phys. Rev. A **18**, 1652 (1978).
[10] Yu.S. Kivshar and B.A. Malomed, Rev. Mod. Phys. **61**, 763 (1989).
[11] P.S. Lomdahl, J. Stat. Phys. **39**, 551 (1985).
[12] M.G. Forest and D.W. McLaughlin, J. Math. Phys. **23**, 1248 (1982).
[13] R.K. Dodd, J.C. Eilbeck, J.D. Gibbon, and H.C. Morris, *Solitons and Nonlinear Wave Equations* (Academic, London, 1982).
[14] A. Barone, F. Esposito, K.K. Likharev, V.K. Semenov, B.N. Todorov, and R. Vaglio, J. Appl. Phys. **53**, 5802 (1982).
[15] G. Carapella, G. Costabile, S. Sakai, and N.F. Pedersen, Phys. Rev. B **58**, 6497 (1998).